The HKU Scholars Hub   The University of Hong Kong   香港大學學術庫

Title	Measurements of the mass and width of the c using the decay (3686) c

Measurements of the Mass and Width of the η_c Using the Decay $\psi(3686) \to \gamma\eta_c$

M. Ablikim,[1] M. N. Achasov,[5] D. Alberto,[41] D. J. Ambrose,[38] F. F. An,[1] Q. An,[39] Z. H. An,[1] J. Z. Bai,[1] R. B. Ferroli,[17] Y. Ban,[25] J. Becker,[2] N. Berger,[1] M. B. Bertani,[17] J. M. Bian,[37] E. Boger,[18,*] O. Bondarenko,[19] I. Boyko,[18] R. A. Briere,[3] V. Bytev,[18] X. Cai,[1] A. C. Calcaterra,[17] G. F. Cao,[1] J. F. Chang,[1] G. Chelkov,[18,*] G. Chen,[1] H. S. Chen,[1] H. X. Chen,[1] J. C. Chen,[1] M. L. Chen,[1] S. J. Chen,[23] Y. Chen,[1] Y. B. Chen,[1] H. P. Cheng,[13] Y. P. Chu,[1] D. Cronin-Hennessy,[37] H. L. Dai,[1] J. P. Dai,[1] D. Dedovich,[18] Z. Y. Deng,[1] I. Denysenko,[18,†] M. Destefanis,[41] W. L. Ding,[27] Y. Ding,[21] L. Y. Dong,[1] M. Y. Dong,[1] S. X. Du,[44] J. Fang,[1] S. S. Fang,[1] C. Q. Feng,[39] C. D. Fu,[1] J. L. Fu,[23] Y. Gao,[34] C. Geng,[39] K. Goetzen,[7] W. X. Gong,[1] M. Greco,[41] M. H. Gu,[1] Y. T. Gu,[9] Y. H. Guan,[6] A. Q. Guo,[24] L. B. Guo,[22] Y. P. Guo,[24] Y. L. Han,[1] X. Q. Hao,[1] F. A. Harris,[36] K. L. He,[1] M. He,[1] Z. Y. He,[24] Y. K. Heng,[1] Z. L. Hou,[1] H. M. Hu,[1] J. F. Hu,[6] T. Hu,[1] B. Huang,[1] G. M. Huang,[14] J. S. Huang,[11] X. T. Huang,[27] Y. P. Huang,[1] T. Hussain,[40] C. S. Ji,[39] Q. Ji,[1] X. B. Ji,[1] X. L. Ji,[1] L. K. Jia,[1] L. L. Jiang,[1] X. S. Jiang,[1] J. B. Jiao,[27] Z. Jiao,[13] D. P. Jin,[1] S. Jin,[1] F. F. Jing,[34] N. Kalantar-Nayestanaki,[19] M. Kavatsyuk,[19] W. Kuehn,[35] W. Lai,[1] J. S. Lange,[35] J. K. C. Leung,[33] C. H. Li,[1] Cheng Li,[39] Cui Li,[39] D. M. Li,[44] F. Li,[1] G. Li,[1] H. B. Li,[1] J. C. Li,[1] K. Li,[10] Lei Li,[1] N. B. Li,[22] Q. J. Li,[1] S. L. Li,[1] W. D. Li,[1] W. G. Li,[1] X. L. Li,[27] X. N. Li,[1] X. Q. Li,[24] X. R. Li,[26] Z. B. Li,[31] H. Liang,[39] Y. F. Liang,[29] Y. T. Liang,[35] G. R. Liao,[34] X. T. Liao,[1] B. J. Liu,[32] C. L. Liu,[3] C. X. Liu,[1] C. Y. Liu,[1] F. H. Liu,[28] Fang Liu,[1] Feng Liu,[14] H. Liu,[1] H. B. Liu,[6] H. H. Liu,[12] H. M. Liu,[12] H. W. Liu,[1] J. P. Liu,[42] K. Liu,[6] K. Liu,[25] K. Y. Liu,[21] Q. Liu,[36] S. B. Liu,[39] X. Liu,[20] X. H. Liu,[1] Y. B. Liu,[24] Yong Liu,[1] Z. A. Liu,[1] Zhiqiang Liu,[1] Zhiqing Liu,[1] H. Loehner,[19] G. R. Lu,[11] H. J. Lu,[13] J. G. Lu,[1] Q. W. Lu,[28] X. R. Lu,[6] Y. P. Lu,[1] C. L. Luo,[22] M. X. Luo,[43] T. Luo,[36] X. L. Luo,[1] M. Lv,[1] C. L. Ma,[6] F. C. Ma,[21] H. L. Ma,[1] Q. M. Ma,[1] S. Ma,[1] T. Ma,[1] X. Y. Ma,[1] M. Maggiora,[41] Q. A. Malik,[40] H. Mao,[1] Y. J. Mao,[25] Z. P. Mao,[1] J. G. Messchendorp,[19] J. Min,[1] T. J. Min,[1] R. E. Mitchell,[16] X. H. Mo,[1] N. Yu. Muchnoi,[5] Y. Nefedov,[18] I. B. Nikolaev,[5] Z. Ning,[1] S. L. Olsen,[26] Q. Ouyang,[1] S. P. Pacetti,[17,‡] J. W. Park,[26] M. Pelizaeus,[36] K. Peters,[7] J. L. Ping,[22] R. G. Ping,[1] R. Poling,[37] C. S. J. Pun,[33] M. Qi,[23] S. Qian,[1] C. F. Qiao,[6] X. S. Qin,[1] J. F. Qiu,[1] K. H. Rashid,[40] G. Rong,[1] X. D. Ruan,[9] A. Sarantsev,[18,§] J. Schulze,[2] M. Shao,[39] C. P. Shen,[36,||] X. Y. Shen,[1] H. Y. Sheng,[1] M. R. Shepherd,[16] X. Y. Song,[1] S. Spataro,[41] B. Spruck,[35] D. H. Sun,[1] G. X. Sun,[1] J. F. Sun,[11] S. S. Sun,[1] X. D. Sun,[1] Y. J. Sun,[39] Y. Z. Sun,[1] Z. J. Sun,[1] Z. T. Sun,[39] C. J. Tang,[29] X. Tang,[1] E. H. Thorndike,[38] H. L. Tian,[1] D. Toth,[37] G. S. Varner,[36] B. Wang,[9] B. Q. Wang,[25] K. Wang,[1] L. L. Wang,[1] L. L. Wang,[4] L. S. Wang,[1] M. Wang,[27] P. Wang,[1] P. L. Wang,[1] Q. Wang,[1] Q. J. Wang,[1] S. G. Wang,[25] X. F. Wang,[11] X. L. Wang,[39] Y. D. Wang,[39] Y. F. Wang,[1] Y. Q. Wang,[27] Z. Wang,[1] Z. G. Wang,[1] Z. Y. Wang,[1] D. H. Wei,[8] Q. G. Wen,[39] S. P. Wen,[1] U. Wiedner,[2] L. H. Wu,[1] N. Wu,[1] W. Wu,[24] Z. Wu,[1] Z. J. Xiao,[22] Y. G. Xie,[1] Q. L. Xiu,[1] G. F. Xu,[1] G. M. Xu,[25] H. Xu,[1] Q. J. Xu,[10] X. P. Xu,[30] Y. Xu,[24] Z. R. Xu,[39] Z. Xue,[1] L. Yan,[39] W. B. Yan,[39] Y. H. Yan,[15] H. X. Yang,[1] T. Yang,[9] Y. Yang,[14] Y. X. Yang,[8] H. Ye,[1] M. Ye,[1] M. H. Ye,[4] B. X. Yu,[1] C. X. Yu,[24] S. P. Yu,[27] C. Z. Yuan,[1] W. L. Yuan,[22] Y. Yuan,[1] A. A. Zafar,[40] A. Z. Zallo,[17] Y. Zeng,[15] B. X. Zhang,[1] B. Y. Zhang,[1] C. C. Zhang,[1] D. H. Zhang,[1] H. H. Zhang,[31] H. Y. Zhang,[1] J. Zhang,[22] J. Q. Zhang,[1] J. W. Zhang,[1] J. Y. Zhang,[1] J. Z. Zhang,[1] L. Zhang,[23] S. H. Zhang,[1] T. R. Zhang,[22] X. J. Zhang,[1] X. Y. Zhang,[27] Y. Zhang,[1] Y. H. Zhang,[1] Y. S. Zhang,[9] Z. P. Zhang,[39] Z. Y. Zhang,[42] G. Zhao,[1] H. S. Zhao,[1] Jingwei Zhao,[1] Lei Zhao,[39] Ling Zhao,[1] M. G. Zhao,[24] Q. Zhao,[1] S. J. Zhao,[44] T. C. Zhao,[1] X. H. Zhao,[23] Y. B. Zhao,[1] Z. G. Zhao,[39] A. Zhemchugov,[18,*] B. Zheng,[1] J. P. Zheng,[1] Y. H. Zheng,[6] Z. P. Zheng,[1] B. Zhong,[1] J. Zhong,[2] L. Zhou,[1] X. K. Zhou,[6] X. R. Zhou,[39] C. Zhu,[1] K. Zhu,[1] K. J. Zhu,[1] S. H. Zhu,[1] X. L. Zhu,[34] X. W. Zhu,[1] Y. S. Zhu,[1] Z. A. Zhu,[1] J. Zhuang,[1] B. S. Zou,[1] J. H. Zou,[1] and J. X. Zuo[1]

(BESIII Collaboration)

[1]*Institute of High Energy Physics, Beijing 100049, People's Republic of China*
[2]*Bochum Ruhr-University, 44780 Bochum, Germany*
[3]*Carnegie Mellon University, Pittsburgh, Pennsylvania 15213, USA*
[4]*China Center of Advanced Science and Technology, Beijing 100190, People's Republic of China*
[5]*G.I. Budker Institute of Nuclear Physics SB RAS (BINP), Novosibirsk 630090, Russia*
[6]*Graduate University of Chinese Academy of Sciences, Beijing 100049, People's Republic of China*
[7]*GSI Helmholtzcentre for Heavy Ion Research GmbH, D-64291 Darmstadt, Germany*
[8]*Guangxi Normal University, Guilin 541004, People's Republic of China*
[9]*GuangXi University, Nanning 530004, People's Republic of China*
[10]*Hangzhou Normal University, Hangzhou, 310036, People's Republic of China*
[11]*Henan Normal University, Xinxiang 453007, People's Republic of China*
[12]*Henan University of Science and Technology, Luoyang 471003, People's Republic of China*

[13]*Huangshan College, Huangshan 245000, People's Republic of China*
[14]*Huazhong Normal University, Wuhan 430079, People's Republic of China*
[15]*Hunan University, Changsha 410082, People's Republic of China*
[16]*Indiana University, Bloomington, Indiana 47405, USA*
[17]*INFN Laboratori Nazionali di Frascati, Frascati, Italy*
[18]*Joint Institute for Nuclear Research, 141980 Dubna, Russia*
[19]*KVI/University of Groningen, 9747 AA Groningen, The Netherlands*
[20]*Lanzhou University, Lanzhou 730000, People's Republic of China*
[21]*Liaoning University, Shenyang 110036, People's Republic of China*
[22]*Nanjing Normal University, Nanjing 210046, People's Republic of China*
[23]*Nanjing University, Nanjing 210093, People's Republic of China*
[24]*Nankai University, Tianjin 300071, People's Republic of China*
[25]*Peking University, Beijing 100871, People's Republic of China*
[26]*Seoul National University, Seoul, 151-747 Korea*
[27]*Shandong University, Jinan 250100, People's Republic of China*
[28]*Shanxi University, Taiyuan 030006, People's Republic of China*
[29]*Sichuan University, Chengdu 610064, People's Republic of China*
[30]*Soochow University, Suzhou 215006, People's Republic of China*
[31]*Sun Yat-Sen University, Guangzhou 510275, People's Republic of China*
[32]*The Chinese University of Hong Kong, Shatin, N.T., Hong Kong*
[33]*The University of Hong Kong, Pokfulam, Hong Kong*
[34]*Tsinghua University, Beijing 100084, People's Republic of China*
[35]*Universitaet Giessen, 35392 Giessen, Germany*
[36]*University of Hawaii, Honolulu, Hawaii 96822, USA*
[37]*University of Minnesota, Minneapolis, Minnesota 55455, USA*
[38]*University of Rochester, Rochester, New York 14627, USA*
[39]*University of Science and Technology of China, Hefei 230026, People's Republic of China*
[40]*University of the Punjab, Lahore-54590, Pakistan*
[41]*University of Turin and INFN, Turin, Italy*
[42]*Wuhan University, Wuhan 430072, People's Republic of China*
[43]*Zhejiang University, Hangzhou 310027, People's Republic of China*
[44]*Zhengzhou University, Zhengzhou 450001, People's Republic of China*

The mass and width of the lowest-lying S-wave spin singlet charmonium state, the η_c, are measured using a data sample of 1.06×10^8 $\psi(3686)$ decays collected with the BESIII detector at the BEPCII storage ring. We use a model that incorporates full interference between the signal reaction, $\psi(3686) \rightarrow \gamma\eta_c$, and a nonresonant radiative background to describe the line shape of the η_c successfully. We measure the η_c mass to be $2984.3 \pm 0.6 \pm 0.6$ MeV/c^2 and the total width to be $32.0 \pm 1.2 \pm 1.0$ MeV, where the first errors are statistical and the second are systematic.

In recent years, many new charmonium or charmoniumlike states have been discovered. These states have led to a revived interest in improving the quark-model picture of hadrons [1]. Even with these new discoveries, the mass and width of the lowest lying charmonium state, the η_c, continue to have large uncertainties when compared to those of other charmonium states [2]. Early measurements of the properties of the η_c using J/ψ radiative transitions [3,4] found a mass and width near 2978 MeV/c^2 and 10 MeV, respectively. However, recent experiments, including photon-photon fusion and B decays, have reported a significantly higher mass and a much larger width [5–8]. The most recent study by the CLEO-c experiment [9], using both $\psi(3686) \rightarrow \gamma\eta_c$ and $J/\psi \rightarrow \gamma\eta_c$, pointed out a distortion of the η_c line shape in $\psi(3686)$ decays. CLEO-c attributed the η_c line-shape

distortion to the energy dependence of the $M1$ transition matrix element.

In this Letter, we report measurements of the η_c mass and width using the radiative transition $\psi(3686) \rightarrow \gamma\eta_c$. We successfully describe the measured η_c line shapes using a combination of the energy dependence of the hindered-$M1$ transition matrix element and a full interference with nonresonant $\psi(3686)$ radiative decays. The analysis is based on a $\psi(3686)$ data sample of 1.06×10^8 events [10] collected with the BESIII detector operating at the BEPCII e^+e^- collider. A 42 pb^{-1} continuum data sample, taken at a center-of-mass energy of 3.65 GeV, is used to measure non-$\psi(3686)$ backgrounds.

The η_c mass and width are determined from fits to the invariant mass spectra of exclusive η_c decay modes. Six modes are used to reconstruct the η_c: $K_S K^+ \pi^-$, $K^+ K^- \pi^0$,

$\eta\pi^+\pi^-$, $K_S K^+\pi^+\pi^-\pi^-$, $K^+K^-\pi^+\pi^-\pi^0$, and $3(\pi^+\pi^-)$, where the K_S is reconstructed in $\pi^+\pi^-$, and the η and π^0 in $\gamma\gamma$ decays. The inclusion of charge conjugate modes is implied.

The BESIII detector is described in detail in Ref. [11]. The detector has a geometrical acceptance of 93% of 4π. A small cell helium-based main drift chamber provides momentum measurements of charged particles; in a 1 T magnetic field the resolution is 0.5% at 1 GeV/c. It also supplies an energy loss ($-dE/dx$) measurement with a resolution better than 6% for electrons from Bhabha scattering. The electromagnetic calorimeter (EMC) measures photon energies with a resolution of 2.5% (5%) at 1 GeV in the barrel (endcaps). The time-of-flight system (TOF) is composed of plastic scintillators with a time resolution of 80 ps (110 ps) in the barrel (endcap) and is mainly useful for particle identification. The muon system provides a 2 cm position resolution and measures muon tracks with momenta greater than 0.5 GeV/c.

We use inclusive Monte Carlo (MC) simulated events as an aid in our background studies. The $\psi(3686)$ resonance is produced by the event generator KKMC [12], while the decays are generated by EVTGEN [13] with known branching fractions [2], or by LUNDCHARM [14] for unmeasured decays. The signal is generated with an angular distribution of $1+\cos^2\theta_\gamma$ for $\psi(3686)\to\gamma\eta_c$, and phase space for multibody η_c decays, where θ_γ is the angle between the photon and the positron beam direction in the center-of-mass system. Simulated events are processed using GEANT4 [15], where measured detector resolutions are incorporated.

We require that each charged track (except those from K_S decays) be consistent with originating from within 1 cm in the radial direction and 10 cm along the beam direction of the run-by-run-determined interaction point. The tracks must be within the main drift chamber fiducial volume, $|\cos\theta|<0.93$. Information from the TOF and $-dE/dx$ is combined to form a likelihood $\mathcal{L}_\pi$ (or $\mathcal{L}_K$) for a pion (or kaon) hypothesis. To identify a track as a pion (kaon), the likelihood $\mathcal{L}_\pi$ ($\mathcal{L}_K$) is required to be greater than 0.1% and greater than $\mathcal{L}_K$ ($\mathcal{L}_\pi$).

Photons are reconstructed from isolated showers in the EMC that are at least 20 degrees away from charged tracks. The energy deposited in the nearby TOF scintillator is included to improve the reconstruction efficiency and the energy resolution. Photon energies are required to be greater than 25 MeV in the fiducial EMC barrel region ($|\cos\theta|<0.8$) and 50 MeV in the endcap ($0.86<|\cos\theta|<0.92$). The showers close to the boundary are poorly reconstructed and excluded from the analysis. Moreover, the EMC timing, with respect to the collision, of the photon candidate must be in coincidence with collision events, i.e., $0\le t\le 700$ ns, to suppress electronic noise and energy deposits unrelated to the event.

The $K_S\to\pi^+\pi^-$ candidates are reconstructed from pairs of oppositely charged tracks. The secondary vertex constrained tracks must have an invariant mass ± 10 MeV/c^2 of the nominal K_S mass, and a decay length more than twice the vertex resolution. The track information at the secondary vertex is an input to the kinematic fit. Candidate π^0 and η mesons are reconstructed from pairs of photons with an invariant mass in the range 0.118 GeV/$c^2 < M(\gamma\gamma) < 0.150$ GeV/c^2 for π^0 and 0.50 GeV/$c^2 < M(\gamma\gamma) < 0.58$ GeV/c^2 for η. The remaining photons are considered as candidates of the transition photon.

Events with either extra charged tracks or nonzero net charge are rejected. The η_c candidates are reconstructed from $K_S K^+\pi^-$, $K^+K^-\pi^0$, $\eta\pi^+\pi^-$, $K_S K^+\pi^+\pi^-\pi^-$, $K^+K^-\pi^+\pi^-\pi^0$, and $3(\pi^+\pi^-)$. We select events in the region 2.7 GeV/$c^2 < M(\eta_c) < 3.2$ GeV/c^2. A four-constraint (4C) kinematic fit of all selected charged particles and the transition photon with respect to the initial $\psi(3686)$ four-momentum is performed to reduce background and improve the mass resolution. When additional photons are found in an event, we loop over all possible combinations and keep the one with the best χ^2_{4C} from the kinematic fit. The χ^2_{4C} is required to be less than 60, a value is determined by optimizing the figure of merit for most of the channels, $S/\sqrt{S+B}$, where $S(B)$ is the number of signal (background) events in the signal region [2.9 GeV/$c^2 < M(\eta_c) < 3.05$ GeV/c^2]. In addition, to remove $\psi(3686)\to\pi^+\pi^-J/\psi$ events, we require there be no $\pi^+\pi^-$ pair with a recoil mass in the J/ψ signal region. To suppress background from $\pi^0\to\gamma\gamma$, we demand that the transition photon should not form a π^0 with any other photon in the event.

The main source of background is from $\psi(3686)\to\pi^0 X_i$ decays, where a photon from the $\pi^0\to\gamma\gamma$ decay is missing, and X_i represents the η_c final states under study. These decays could proceed via various intermediate states, and most of the branching fractions are unknown. To estimate their contribution, we reconstruct $\psi(3686)\to\pi^0 X_i$ decays from data. The selection criteria are similar to those applied to the $\gamma\eta_c$ candidates except an additional photon is required. The $\psi(3686)\to\pi^0 X_i$ signal yields are extracted from fits to the $M(\gamma\gamma)$ invariant mass distributions for different $M(X_i)$ mass bins. The relative efficiencies of the $\gamma\eta_c$ and $\pi^0 X_i$ selection criteria are estimated in each $M(X_i)$ mass bin using phase space distributed $\psi(3686)\to\pi^0 X_i$ MC events. Combining this relative efficiency with the number of $\psi(3686)\to\pi^0 X_i$ signal events in every $M(X_i)$ bin, we estimate the $\pi^0 X_i$ events that pass the $\gamma\eta_c$ selection. We also examine the efficiencies of $\pi^0 X_i$ events generated with different dynamics, and the change is negligible.

Other potential $\psi(3686)$ decay backgrounds are investigated using 1.06×10^8 inclusive MC events where $\pi^0 X_i$ events have been excluded. We find no other dominant

background processes, but do find dozens of decay modes that each make small additional contributions to the background. These decays typically have additional or fewer photons in their final states. The sum of these background events is used to estimate the contribution from other $\psi(3686)$ decays. Backgrounds from the $e^+ e^- \to q\bar{q}$ continuum process are studied using a data sample taken at $\sqrt{s} = 3.65$ GeV. Continuum backgrounds are found to be small and uniformly distributed in $M(X_i)$. There is also an irreducible nonresonant background, $\psi(3686) \to \gamma X_i$, that has the same final state as signal events. A nonresonant component is included in the fit to the η_c invariant mass.

Figure 1 shows the η_c invariant mass distributions for selected η_c candidates, together with the estimated $\pi^0 X_i$ backgrounds, the continuum backgrounds normalized by luminosity, and other $\psi(3686)$ decay backgrounds estimated from the inclusive MC sample. A clear η_c signal is evident in every decay mode. We note that all of the η_c signals have an obviously asymmetric shape: there is a long tail on the low-mass side; while on the high-mass side, the signal drops rapidly and the data dips below the expected level of the smooth background. This behavior of the signal suggests possible interference with the nonresonant γX_i amplitude. In this analysis, we assume 100% of the nonresonant amplitude interferes with the η_c.

The solid curves in Fig. 1 show the results of an unbinned simultaneous maximum likelihood fit in the range from 2.7 to 3.2 GeV/c^2 with three components: signal, nonresonant background, and a combined background consisting of $\pi^0 X_i$ decays, continuum, and other $\psi(3686)$ decays. The signal is described by a Breit-Wigner function convolved with a resolution function. The nonresonant amplitude is real, and is described by an expansion to second order in Chebyshev polynomials defined and normalized over the fitting range. The combined background is fixed at its expected intensity, as described earlier. The fitting probability density function as a function of mass (m) reads

$$F(m) = \sigma \otimes [\epsilon(m)|e^{i\phi} E_\gamma^{7/2} \mathcal{S}(m) + \alpha \mathcal{N}(m)|^2] + \mathcal{B}(m),$$

where $\mathcal{S}(m)$, $\mathcal{N}(m)$, and $\mathcal{B}(m)$ are the signal, the nonresonant γX_i component, and the combined background, respectively; E_γ is the photon energy, σ is the experimental resolution, and $\epsilon(m)$ is the mass-dependent efficiency. The E_γ^7 multiplying $|\mathcal{S}(m)|^2$ reflects the expected energy dependence of the hindered-$M1$ transition [16], which partially contributes to the η_c low-mass tail as well as the interference effect. The interference phase ϕ and the strength of the nonresonant component α are allowed to vary in the fit.

The mass-dependent efficiencies are determined from phase space distributed MC simulations of the η_c decays. Efficiencies obtained from MC samples that include intermediate states change the resulting mass and width by negligible amounts. MC studies indicate that the resolution is almost constant over the fitting range. Thus, a mass-independent resolution is used in the fit. The detector resolution is primarily determined by MC simulation for
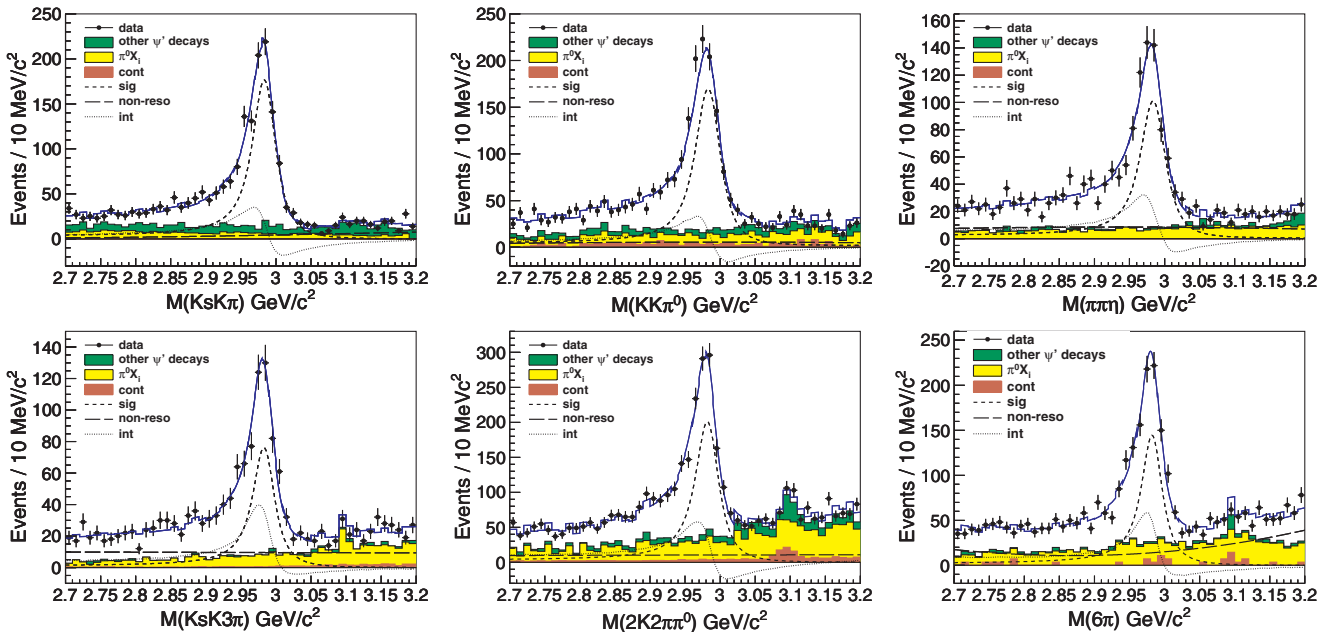

FIG. 1 (color). The $M(X_i)$ invariant mass distributions for the decays $K_S K^+ \pi^-$, $K^+ K^- \pi^0$, $\eta \pi^+ \pi^-$, $K_S K^+ \pi^+ \pi^- \pi^-$, $K^+ K^- \pi^+ \pi^- \pi^0$, and $3(\pi^+ \pi^-)$, respectively, with the fit results (for the constructive solution) superimposed. Points are data and the various curves are the total fit results. Signals are shown as short-dashed lines, the nonresonant components as long-dashed lines, and the interference between them as dotted lines. Shaded histograms are (in red, yellow, green) for [continuum, $\pi^0 X_i$, other $\psi(3686)$ decays] backgrounds. The continuum backgrounds for $K_S K^+ \pi^-$ and $\eta \pi^+ \pi^-$ decays are negligible.

each η_c decay mode. The consistency between the data and MC simulation is checked by the decay $\psi(3686) \rightarrow \gamma\gamma J/\psi$, where the J/ψ decays into the same final states as the η_c. We use a smearing Gaussian function to describe possible discrepancies between data and MC. By fitting the MC-determined J/ψ shape convolved by a smearing Gaussian function to the data, we determine the parameters of the Gaussian function. Because of the different kinematics, the parameters are slightly different for each mode.

In the simultaneous fit, the η_c mass and width are constrained to be the same for all the decay modes but still free parameters; the two Chebyshev polynomial coefficients and the factor α are also allowed to float. Two solutions for the relative phase are found for each decay mode, one corresponds to constructive and the other destructive interference between the two amplitudes at the η_c peak. Regardless of which solution we take, the mass, width of the η_c, and the overall fit quality are always unchanged [17]. The mass is $M = 2984.3 \pm 0.6$ MeV/c^2, and the width is $\Gamma = 32.0 \pm 1.2$ MeV. The goodness of fit is $\chi^2/ndf = 283.4/274$, which indicates a reasonable fit. The solutions for the relative phase of each mode are listed in Table I.

However, without the interference term, the fit would miss some data points, especially where the symmetric shape of a Breit-Wigner function is deformed, and the goodness of fit is $\chi^2/ndf = 426.6/280$. The statistical significance of the interference, calculated based on the differences of likelihood and degrees of freedom between fits with and without interference, is of order 15σ.

The systematic uncertainties of the η_c mass and width mainly come from the background estimation, the mass scale and resolution, the shape of the nonresonant component, the fitting range, and the efficiency.

In the fit, the $\pi^0 X_i$ background is fixed at its expected intensity, so the statistical uncertainty of the observed $\pi^0 X_i$ events introduces a systematic error. To estimate this uncertainty, we vary the number of events in each bin by assuming Gaussian variations from the expected value. We repeat this procedure a thousand times, and take the standard deviation of the resulting mass, width, and phases as systematic errors. We also use different dynamics in generating the $\pi^0 X_i$ events (with the same final state, but

different intermediate states) for the efficiency correction, and find the differences in resulting mass and width are small. We take 0.24 MeV/c^2 in mass and 0.44 MeV in width as the systematic errors for the $\pi^0 X_i$ background estimation.

We assign a 0.07 MeV/c^2 (0.06 MeV) error in mass (width) for the nonresonant component shape that is obtained by changing the polynomial order. Also we include an additional noninterfering component, which is represented by a 2nd-order polynomial with free strength and shape parameters. The changes in the resulting η_c mass and width are 0.10 MeV/c^2 and 0.02 MeV, respectively, and the fraction of this component to the total nonresonant rate varies from 0 to 25% depending on the decay mode. These variations are included in systematic errors.

The systematic error from the uncertainty in the other $\psi(3686)$ decay backgrounds is estimated by floating the magnitude and changing the shape of this component to a 2nd-order polynomial with free parameters. The changes, 0.05 MeV/c^2 in mass and 0.06 MeV in width, are taken as systematic errors.

The consistency of the mass scale and resolution between data and MC simulations is checked with the decay $\psi(3686) \rightarrow \gamma\gamma J/\psi$, and possible discrepancies are described by a smearing Gaussian distribution, where a nonzero mean value indicates a mass offset, and a nonzero σ represents the difference between the data and MC mass resolutions $(\sigma_{\text{data}}^2 - \sigma_{\text{MC}}^2)^{1/2}$. A typical mass shift is about -1.0 MeV/c^2 and the resolution smear is ~ 3.0 MeV. Another possible bias is the difference between input and the value after event reconstruction and selection. This is small for both the mass shift (< 0.3 MeV) and resolution smear. Both of these are added in the smearing Gaussian distribution. By varying the parameters of the smearing Gaussian distribution from the expected value, we estimate the uncertainties. From a large number of tests, the standard deviation of the resulting mass (width), 0.38 MeV/c^2 (0.27 MeV), is taken as a systematic error in mass (width) for the mass scale uncertainty. A 0.35 MeV/c^2 (0.60 MeV) systematic error in mass (width) is assigned due to the mass resolution uncertainty.

The systematic error due to the fitting range is estimated by varying the lower end between 2.6 and 2.8 GeV/c^2 and the higher end between 3.1 and 3.3 GeV/c^2. The changes, 0.05 MeV/c^2 in mass and 0.07 MeV in width, are assigned as systematic errors. A mass-dependent efficiency is used in the fit. By removing the efficiency correction from the fitting probability density function, the changes, which are 0.05 MeV/c^2 in mass and 0.06 MeV in width, are taken as systematic errors. The stability of the simultaneous fit program is checked by repeating the fit a thousand times with random initialization; the standard deviation of mass and width, 0.14 MeV/c^2 and 0.66 MeV, respectively, are taken as systematic errors.

TABLE I. Solutions of the relative phase (in unit of radian) of each decay mode.

Mode	Constructive	Destructive
$K_S K^+ \pi^-$	2.94 ± 0.27	3.75 ± 0.26
$K^+ K^- \pi^0$	2.63 ± 0.21	3.96 ± 0.19
$\eta \pi^+ \pi^-$	2.41 ± 0.13	4.28 ± 0.09
$K_S K^+ \pi^+ \pi^-$	2.16 ± 0.11	4.46 ± 0.07
$K^+ K^- \pi^+ \pi^- \pi^0$	2.73 ± 0.19	4.00 ± 0.16
$3(\pi^+ \pi^-)$	2.28 ± 0.10	4.43 ± 0.06

We assume all these sources are independent and take their sum in quadrature as the total systematic error. We obtain the η_c mass and width to be

$$M = 2984.3 \pm 0.6 \pm 0.6 \text{ MeV}/c^2,$$

$$\Gamma = 32.0 \pm 1.2 \pm 1.0 \text{ MeV}.$$

Here (and elsewhere) the first errors are statistical and the second are systematic.

The relative phases for constructive interference or destructive interference from each mode are consistent with each other within 3σ, which may suggest a common phase in all the modes under study. A fit with a common phase (i.e., the phases are constrained to be the same) describes the data well, with a $\chi^2/ndf = 303.2/279$. Comparing to the fit with separately varying phases for each mode, we find the statistical significance for the case of five distinct phases to be 3.1σ. This fit yields $M = 2983.9 \pm 0.6 \pm 0.6 \text{ MeV}/c^2$, $\Gamma = 31.3 \pm 1.2 \pm 0.9 \text{ MeV}$, and $\phi = 2.40 \pm 0.07 \pm 0.47$rad (constructive) or $\phi = 4.19 \pm 0.03 \pm 0.47$rad (destructive). The physics behind this possible common phase is yet to be understood.

In summary, we measure the η_c mass and width via $\psi(3686) \to \gamma\eta_c$ by assuming all radiative nonresonant events interfere with the η_c. These results are so far the most precise single measurement of the mass and width of η_c [2]. For the first time, interference between the η_c and the nonresonant amplitudes around the η_c mass is considered; given the assumptions of our fit, the significance of the interference is of order 15σ. We note that this interference affects the η_c mass and width significantly, and may have impacted all of the previous measurements of the η_c mass and width that used radiative transitions. Our results are consistent with those from photon-photon fusion and B decays [5–8]; this may partly clarify the discrepancy puzzle discussed above. The changes of the η_c mass and width may also have an impact on the expected η_c' mass and width, and will modify the parameters used in charmonium potential models, where the η_c mass is one of the input parameters. From this measurement, we determine the hyperfine mass splitting to be $\Delta M_{\text{hf}}(1S)_{c\bar{c}} \equiv M(J/\psi) - M(\eta_c) = 112.6 \pm 0.8 \text{ MeV}/c^2$, which agrees well with recent lattice computations [18–20] as well as quark-model predictions [21], and sheds light on spin-dependent interactions in quarkonium states.

*Also at the Moscow Institute of Physics and Technology, Moscow, Russia.
†On leave from the Bogolyubov Institute for Theoretical Physics, Kiev, Ukraine.
‡Currently at University of Perugia and INFN, Perugia, Italy.
§Also at the PNPI, Gatchina, Russia.
‖Now at Nagoya University, Nagoya, Japan.
[1] See, for example, E. S. Swanson, Phys. Rep. **429**, 243 (2006); E. Klempt and A. Zaitsev, Phys. Rep. **454**, 1 (2007); S. Godfrey and S. L. Olsen, Annu. Rev. Nucl. Part. Sci. **58**, 51 (2008); N. Brambilla *et al.*, Eur. Phys. J. C **71**, 1534 (2011).
[2] K. Nakamura *et al.* (Particle Data Group), J. Phys. G **37**, 075021 (2010).
[3] R. M. Baltrusaitis *et al.* (Mark-III Collaboration), Phys. Rev. D **33**, 629 (1986).
[4] J. Z. Bai *et al.* (BES Collaboration), Phys. Lett. B **555**, 174 (2003).
[5] D. M. Asner *et al.* (CLEO Collaboration), Phys. Rev. Lett. **92**, 142001 (2004).
[6] B. Aubert *et al.* (*BABAR* Collaboration), Phys. Rev. Lett. **92**, 142002 (2004).
[7] S. Uehara *et al.* (Belle Collaboration), Eur. Phys. J. C **53**, 1 (2008).
[8] A. Vinokurova *et al.* (Belle Collaboration), Phys. Lett. B **706**, 139 (2011).
[9] R. E. Mitchell *et al.* (CLEO Collaboration), Phys. Rev. Lett. **102**, 011801 (2009).
[10] M. Ablikim *et al.* (BESIII Collaboration), Phys. Rev. D **81**, 052005 (2010).
[11] M. Ablikim *et al.* (BESIII Collaboration), Nucl. Instrum. Methods Phys. Res., Sect. A **614**, 345 (2010).
[12] S. Jadach, B. F. L. Ward, and Z. Was, Comput. Phys. Commun. **130**, 260 (2000); Phys. Rev. D **63**, 113009 (2001).
[13] R. G. Ping *et al.*, Chinese Phys. C **32**, 243 (2008); http://www.slac.stanford.edu/~lange/EvtGen/
[14] J. C. Chen, G. S. Huang, X. R. Qi, D. H. Zhang, and Y. S. Zhu, Phys. Rev. D **62**, 034003 (2000).

[15] S. Agostinelli *et al.* (GEANT4 Collaboration), Nucl. Instrum. Methods Phys. Res., Sect. A **506**, 250 (2003).

[16] N. Brambilla, Y. Jia, and A. Vairo, Phys. Rev. D **73**, 054005 (2006).

[17] K. Zhu, X. H. Mo, C. Z. Yuan, and P. Wang, Int. J. Mod. Phys. A **26**, 4511 (2011).

[18] T. Burch *et al.*, Phys. Rev. D **81**, 034508 (2010).

[19] L. Levkova and C. DeTar, Phys. Rev. D **83**, 074504 (2011).

[20] T. Kawanai and S. Sasaki, arXiv:1110.0888 [Phys. Rev. D (to be published)].

[21] K. K. Seth, arXiv:0912.2776v1.